Available online at www.sciencedirect.com
SCIENCE DIRECT®
International Journal of Mass Spectrometry 242 (2005) 57–62
International Journal of Mass Spectrometry
www.elsevier.com/locate/ijms

Gas phase antimony/tungsten/oxygen cluster cations

Tsunehiko Fujiwara, Akiko Iizuka, Koken Sato, Yasuhiro Yamada*

Department of Chemistry, Tokyo University of Science, 1–3 Kagurazaka, Shinjuku-ku, Tokyo 162-8601, Japan

Received 1 July 2004; accepted 29 November 2004
Available online 28 December 2004

Abstract

Sb/W/O cluster ions were produced using a gas-aggregation source and were investigated by time-of-flight mass spectrometry following ionization with a 266-nm YAG laser. A W-heater in the presence of O_2 gas and Sb vapor reacted to produce the Sb/W/O species, followed by ionization and fragmentation to produce stable cluster ions which could be observed in mass spectra. Two series of cluster ions, $(Sb_3O_4)(WO_3)_n^+$ and $(Sb_5O_7)(WO_3)_n^+$, were found to be stable along with cluster ions with a balanced count of free valence electrons. The cluster structures were estimated by density-functional calculations.

Keywords: Antimony; Tungsten; Oxide; Cluster ion; Time-of-flight mass spectrometry

1. Introduction

Group 15 metals are semi-metals in the bulk form, and metals such as Sb and As exist as different allotropic structures in the bulk form. Sb clusters have been produced in the gas phase and their magic numbers indicate tetrahedral packing structures [1]. Fragmentation or evaporation experiments have shown that antimony clusters have the form Sb_4 [2,3]. The crystalline structures of Sb_4 molecules have been observed in the condensed phase using scanning tunneling microscopy [4]. Antimony cluster ions, Sb_n^+, obtained after fragmentation following ionization with a large excess of energy, have a deltahedron structure and their stability is explained by Wade's rule or polyhedral skeletal electronic pair theory (PSEPT) [5]. Among oxides of the group 15 elements, P and As mainly form molecular oxides, whereas Sb and Bi tend to form polymeric oxide structures. Theoretical calculations of small antimony clusters have been reported [6]. Antimony oxide cluster ions have been produced by gas aggregation [7,8] and laser ablation sources [9]. Antimony oxide cluster ions have also been produced by a pulsed arc cluster ion source (PACIS), in which Sb is vaporized by a high voltage arc-discharge [10–12]. The stability of the cluster ions is explained in terms of minimization of the number of unpaired electrons by the formation of metal–oxygen electron-pair bonds. The gas phase cluster ions $(M_2O_3)_n^+$ and $(M_2O_3)_nMO^+$ (M = Sb, Bi) have been reported [13], reflecting the structure of the bulk solid or the stability resulting from the balanced charge of their valence electrons. Anionic series of antimony oxide clusters [14] and alloy clusters Sb/Mg/O have also been reported [15]. Antimony oxides have attracted attention because of their catalytic properties, especially in combination with other metal oxides [16]. A theoretical study has investigated the reactivity of bismuth oxide cluster cations [17].

In this study, we investigate Sb/W/O cluster ions in order to study the influence of valence electrons from additional atoms (W) on the antimony oxide clusters. Tungsten, W, is a group 6 element with a valence of 6, and as such the Sb/W/O cluster would be expected to have different electronic counts from Sb/O clusters. Generally, it is difficult to obtain W-atom vapor because of its low vapor pressure; tungsten metal has the highest melting point (3683 K) and lowest vapor pressure of all metals. Tungsten and its alloys have been used extensively in industrial applications, such as in filaments, heaters, and numerous spacecraft and high-temperature applications. Tungsten oxide forms various compounds with

* Corresponding author. Tel.: +81 3 5228 8276; fax: +81 3 3235 2214.
E-mail address: yyasu@rs.kagu.tus.ac.jp (Y. Yamada).

1387-3806/$ – see front matter © 2004 Elsevier B.V. All rights reserved.
doi:10.1016/j.ijms.2004.11.015

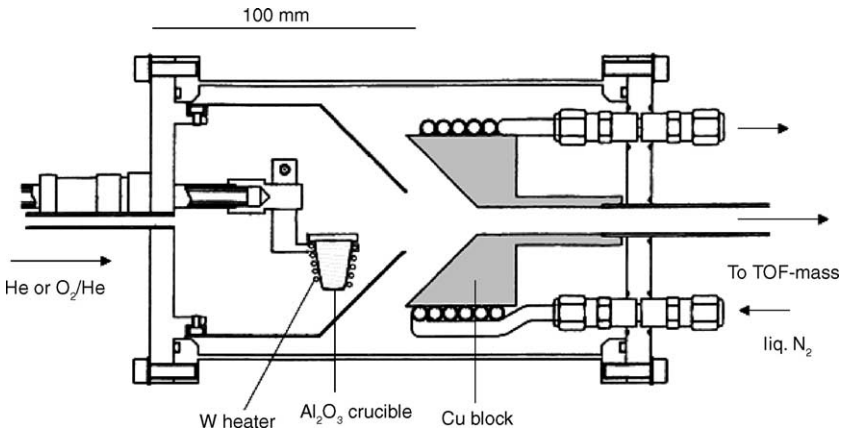

Fig. 1. Gas-aggregation source.

metal elements, and tungstibite, $Sb_2O_3{\cdot}WO_3$, is known as a natural mineral [18]. Although large particles have been studied in a mixture of Bi_2O_3 and WO_3 smoke [19], Sb/W/O cluster ions have yet to be studied.

2. Experimental

A gas-aggregation source was employed for cluster formation as displayed in Fig. 1. Sb shot metal in an alumina crucible was resistively heated and evaporated under a flow of He gas (0.1–1.5 slm (standard $l\,min^{-1}$)). Three tungsten wires (ϕ 0.8 mm) were twisted together and employed as a heater to provide the W-atom source in formation of the Sb/W/O cluster ions. The gas mixture was cooled by a cold Cu block (77 K), resulting in the formation of neutral clusters by aggregation. The reactant gas (O_2) was mixed with the He carrier gas. The gas sample was introduced into an ionization area through two skimmers in combination with a mechanical booster pump and two diffusion pumps. Neutral clusters were then ionized with fourth-harmonic light from a Nd:YAG laser (266 nm, 10 Hz; Minilite-II, HOYA Continuum Corp.). The cluster ions were accelerated in an electric field (1.6 kV), passed through a 45-cm time-of-flight tube, and detected by a micro-channel plate (MCP) in an area evacuated by a turbo molecular pump. The signals from the MCP were captured using a digital oscilloscope (LeCroy 9310A).

3. Results and discussion

Prior to studying the Sb/W/O system, pure Sb cluster ions were obtained in order to observe their distribution. A typical spectrum of Sb_n^+ is shown in Fig. 2. Sb_n^+ cluster ions were observed up to $n = 21$, and Sb_5^+ and Sb_7^+ were found in abundance reflecting their stable structures (magic numbers) as explained by PSEPT; Sb_5^+ and Sb_7^+ correspond to *nido* and *arachno* in Wade's rule, respectively. The mass distribution of the spectrum indicates that the Sb_n^+ cluster ions were produced following fragmentation of larger Sb_m ($m > n$) clusters after ionization, because cluster ions consisting of Sb_4 units are not observed as dominant signals. Under this experimental condition, the mass spectra reflect the stability of the cluster cations rather then the precursor neutral clusters. Cluster ions containing W atoms were not observed in the spectrum as the W metal has a very low vapor pressure and does not generally vaporize at the temperature (<1000 K) of this experiment.

In order to perform oxidation, O_2 was added to the stream of He carrier gas. The mass spectrum of Sb/W/O obtained by adding 20 sccm (standard $cc\,min^{-1}$) of O_2 to a 0.30 slm flow of He carrier gas is shown in Fig. 3. The intensities of oxidized cluster ions decreased when the concentration of O_2 gas was decreased. When the concentration of O_2 was too high (>30 sccm), cluster ion signals were not observed, perhaps due to formation of even larger oxidized particles in the gas-aggregation source. It is known that tungsten oxide, WO_3, is produced by reaction of metallic W with O_2 at high temperature, and that the melting point of WO_3 (1746 K) is much lower than that of W metal (3693 K). When the W wire was resistively heated in the stream of O_2/He gas, WO_3 may have been produced on the surface of the W wire in the presence of O_2, facilitating vaporization of W atoms. However, neither the tungsten oxide cluster nor the tungsten cluster could be detected in the spectrum (Fig. 3). The experiments were also performed without Sb metal. W wire was heated in an empty crucible under a stream of O_2/He, but again, neither the tungsten oxide cluster nor the tungsten cluster was detected. This suggests that neither W atoms nor WO_3 is present in the gas-aggregation source, and that the formation of Sb/W/O clusters is always associated with the vaporization of Sb metal. Therefore, a large Sb/W/O compound produced on the W heater in the presence of O_2 gas and Sb vapor may play an important role as a precursor of the Sb/W/O cluster ions.

In the mass spectrum of the Sb/W/O cluster experiments (Fig. 3), the antimony oxide cluster ions $Sb_3O_4^+$ and $Sb_5O_7^+$ were observed, but $Sb_xO_y^+$ cluster ions of the $(Sb_2O_3)_n^+$ and $(Sb_2O_3)_nSbO^+$ series ($n > 3$) were not observed. Besides these series of antimony oxide cluster ions, $Sb_3WO_7^+$ and

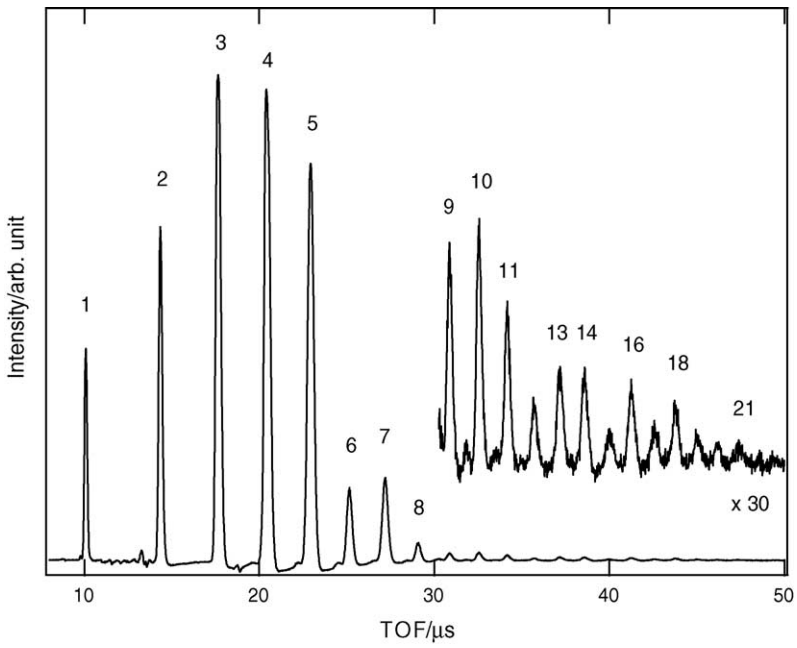

Fig. 2. Time-of-flight mass spectra of Sb_n^+ cluster ions. Numbers correspond to n in Sb_n^+.

$Sb_5WO_{10}^+$ always appeared as intense signals in our experiments, reflecting their peculiar stability. Although the mass of $Sb_3WO_7^+$ is close to that of $Sb_4O_{11}^+$, $Sb_4O_{11}^+$ does not have such a stable geometric or electronic structure. Similarly, the mass of $Sb_5WO_{10}^+$ is close to that of $Sb_6O_{10}^+$. The antimony oxide cluster ions $Sb_4O_{11}^+$ and $Sb_6O_{10}^+$ have not been reported in the literature, and thus it is more reasonable to assign the peaks to members of the Sb/W/O cluster ion series of $(Sb_3O_4)(WO_3)_n^+$ and $(Sb_5O_7)(WO_3)_n^+$ ($n = 1, 2, 3$). These series have balanced numbers of free valence electrons, with valence electron counts of +3, +6, and −2 for Sb, W, and O, respectively. All of the Sb/W/O cluster ions observed in the spectra were members of the series of $(Sb_3O_4)(WO_3)_n^+$ or $(Sb_5O_7)(WO_3)_n^+$. Thus, Sb/W/O cluster ions were stabilized when the total charge was balanced according to the valence electron count of the individual atoms.

In order to examine the effects of oxidizing gas, N_2O was introduced instead of O_2. No essential change was ob-

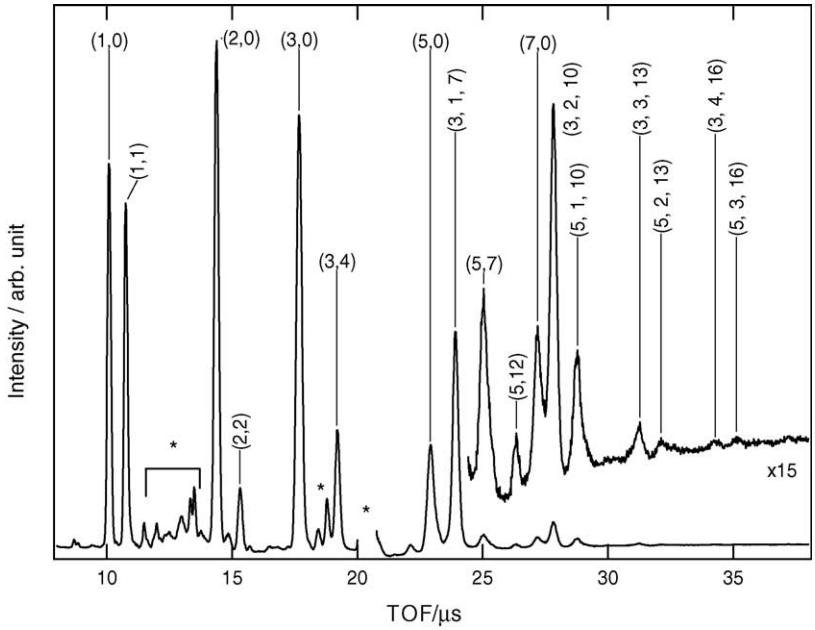

Fig. 3. Time-of-flight mass spectra of Sb/W/O cluster ions. Flow rates of O_2 and He are 20 sccm and 0.30 slm, respectively. Numbers correspond to (x, y) and (p, q, r) in $Sb_xO_y^+$ and $Sb_pW_qO_r^+$, respectively; (*) indicates pump-oil signal.

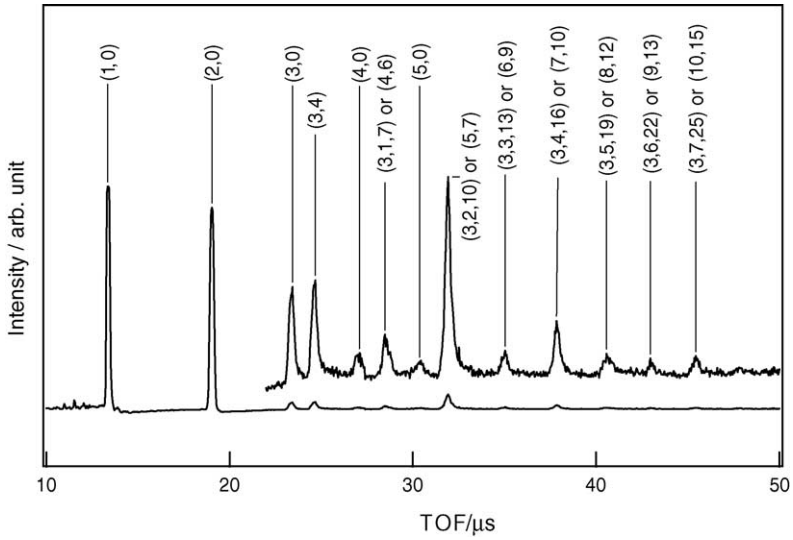

Fig. 4. Time-of-flight mass spectrum of Bi/O and Bi/W/O cluster ions. Bi metal was heated by W-wire. Flow rates of O_2 and He are 17 sccm and 0.35 slm, respectively. Indicated numbers in the figure are (n, m) and (x, y, z) in $Bi_nO_m^+$ and $Bi_xW_yO_z^+$, respectively.

served in the spectral pattern except that the $(Sb_3O_4)(WO_3)_n^+$ and $(Sb_5O_7)(WO_3)_n^+$ intensities became relatively small because of the decreased oxidizing ability of N_2O compared to O_2.

Alternative heater materials to W, including Ta or Mo, were employed in similar experiments. Without introduction of O_2, neat Sb_n^+ clusters were obtained using a Ta or Mo heater and similar mass distributions were revealed in the spectra as those obtained using a W heater. When O_2 was introduced into the gas-aggregation source using a Ta heater, the amount of $Sb_nO_m^+$ or $Sb_xTa_yO_z^+$ cluster ions was too low to be observed in the mass spectrum. Using a Mo heater, small amounts of $Sb_3MoO_7^+$ and $Sb_3O_4^+$ were obtained. Sb/Ta/O or Sb/Mo/O cluster ions could not be effectively produced in the gas-aggregation source using a Ta or Mo heater. The formation of $Sb_xW_yO_z$ species in the gas-aggregation source may assist in the formation of larger $Sb_nO_m^+$ cluster ions and $Sb_xW_yO_z^+$ cluster ions as fragmentation products after ionization.

In order to study similar alloy oxide cluster ions, Bi metal was employed instead of Sb metal. The mass spectrum obtained without introduction of O_2 revealed neat Bi_n^+ cluster ions with a similar distribution to that of the Sb_n^+ cluster ions and with magic numbers of Bi_5^+ and Bi_7^+. A mass spectrum of the Bi/O and Bi/W/O cluster ions is shown in Fig. 4. Bi metal was heated using a W wire, and the flow rates of O_2 and He were 17 sccm and 0.35 slm, respectively. The cluster ions $Bi_3O_4^+$ and $Bi_5O_7^+$ were observed as intense peaks, reflecting the stability derived from the balanced valence electron charge. Cluster ions of the series of $(Bi_2O_3)_nBiO^+$ (n = 1, 2, 3, 4, 5) were also observed. Besides these, $Bi_4O_6^+$ and $Bi_6O_9^+$ of the $(Bi_2O_3)_n^+$ series were obtained, reflecting the structure of the bulk solid. Though the assignments are reasonable without including W atoms, assignments including W atoms are also possible. $(Bi_3O_4)(WO_3)_n^+$ has almost identical mass to $(Bi_2O_3)_nBiO^+$ or $(Bi_2O_3)_n^+$ because Bi_2O_3 = 466.0 and W_2O_6 = 464.0. As such, both assignments are possible.

4. Density-functional calculation

We performed density-functional calculations using the Amsterdam Density Functional (ADF) program package [20] in order to estimate the geometry of the cluster ions and to estimate their stability. As the cluster ions contain heavy atoms (Sb and W), it is preferable to include scalar relativistic effects. Thus, we employed zero order regular approximation (ZORA [21]) calculations with TZP (core double zeta, valence triple zeta, polarized basis sets) in the ADF program. We assumed that all of the Sb/W/O cluster ions were singlet states (S = 0). Optimized structures of $(Sb_3O_4)(WO_3)_n^+$ and $(Sb_5O_7)(WO_3)_n^+$ (n = 0, 1, 2, 3) cluster ions are summarized in Figs. 5 and 6. Ab initio calculations for $Sb_3O_4^+$ and $Sb_5O_7^+$ have been reported in the literature [12], and our calculations for $Sb_3O_4^+$ and $Sb_5O_7^+$ resulted in identical structures in which all of the Sb atoms have three bonds and one of the O atoms forms three bonds. $Sb_3WO_7^+$ has C_{3v} symmetry with the W atom bound opposite a six-membered ring consisting of three Sb and three O atoms. The W atom binds tetrahedrally to four O atoms (WO_4), with one of the O atoms in a terminal position. The structure of $Sb_3WO_7^+$ could result from substitution of the three-bonded O atom in $Sb_3O_4^+$ with a WO_4 unit. In our experiments, $Sb_3WO_7^+$ always appeared as an intense signal in the mass spectra as a result of its high stability. The calculations indicate that it has a highly symmetrical structure, one of the apparent reasons for its high stability. For $Sb_3W_2O_{10}^+$, we performed calculations starting from various initial structures, and the structure shown in Fig. 5c was found to be the most stable. The structure in Fig. 5d is slightly less stable (0.08 eV) than the structure in Fig. 5c. Both of the W

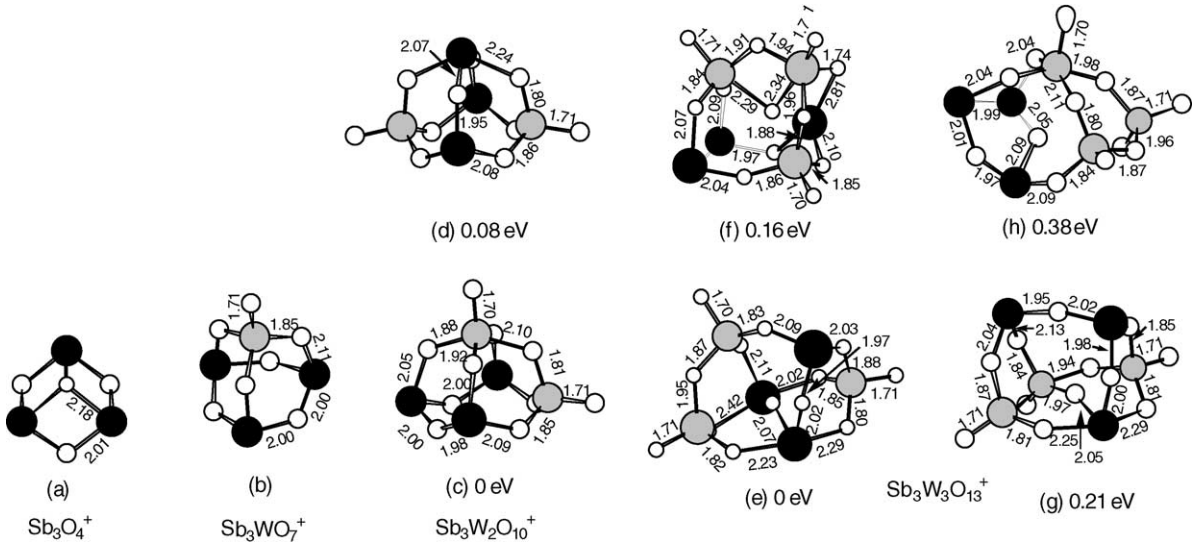

Fig. 5. Optimized structures for $(Sb_3O_4)(WO_3)_n^+$ ($n = 0, 1, 2, 3$) using ADF (ZORA/TZP). Large black balls, large gray balls, and small white balls denote antimony, tungsten, and oxygen, respectively. Relative bond energies are indicated for the species with isomers. Bond lengths are given in angstroms.

atoms in $Sb_3W_2O_{10}^+$ have an O atom in a terminal position. The cluster ion $Sb_3W_2O_{10}^+$ does not have a three-bonded O atom. Several isomers of $Sb_3W_3O_{13}^+$ having similar bonding energies were found (Fig. 5e–h). $Sb_3W_3O_{13}^+$ in Fig. 5e is the most stable cluster ion, in which each W atom has a tetrahedral structure (WO_4) and two of the Sb atoms have four bonds. The isomer in Fig. 5g has a similar structure to Fig. 5e. The $Sb_3W_3O_{13}^+$ isomers tend to have similar structures, with two sets of six-membered rings in which nine O atoms are in bridging positions, though these structures lack symmetry.

The $Sb_5WO_{10}^+$ cluster ion has a structure in which each Sb and W atom is connected to three bridging O atoms, with the Sb atoms having three bonds and the W atom having four bonds with one O in a terminal position. The structure of $Sb_5WO_{10}^+$ could be generated from substitution of the three-bonded O atom in $Sb_5O_7^+$ with a WO_4 unit. The $Sb_5WO_{10}^+$ isomers (Fig. 6j and k) have very similar structures and bonding energies but the distorted structure (Fig. 6j) is more stable. For the larger $Sb_5W_2O_{13}^+$ and $Sb_5W_3O_{16}^+$ cluster ions, structures in which all the W atoms were bound to four O atoms (tetrahedral WO_4) were not obtained as the optimized structures. One of the W atoms in $Sb_5W_2O_{13}^+$ (Fig. 6l) bonds to four O atoms, and another W atom bonds to five O atoms. In a slightly less stable isomer of $Sb_5W_2O_{13}^+$ (Fig. 6m), the two W atoms have six bonds and three of the O atoms have three

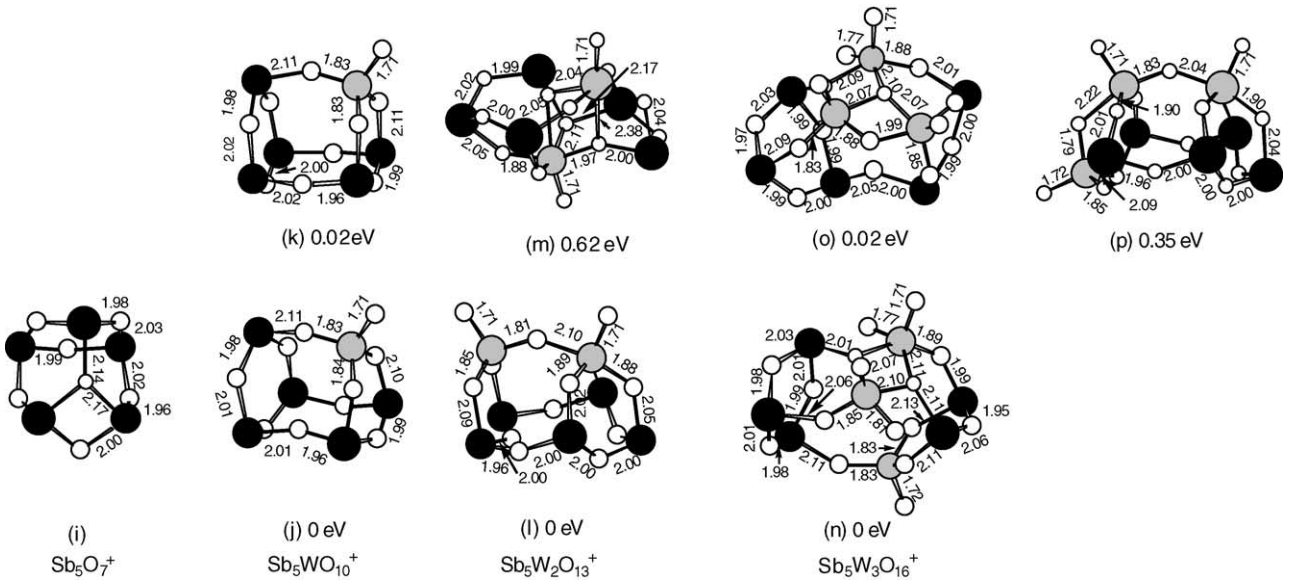

Fig. 6. Optimized structures for $(Sb_5O_7)(WO_3)_n^+$ ($n = 0, 1, 2, 3$) using ADF (ZORA/TZP). Large black balls, large gray balls, and small white balls denote antimony, tungsten, and oxygen, respectively. Relative bond energies are indicated for the species with isomers. Bond lengths are given in angstroms.

bonds. In the most stable $Sb_5W_3O_{16}^+$ structure (Fig. 6n), there are two W atoms with five bonds and one W atom with four bonds. Another isomer of $Sb_5W_3O_{16}^+$ (Fig. 6p) has two W atoms with five bonds and one W atom with four bonds, which may be considered as the product of the addition of a WO_3 unit to $Sb_5W_2O_{13}^+$ (Fig. 6l). The optimized structures of the larger cluster ions $Sb_5W_2O_{13}^+$ and $Sb_5W_3O_{16}^+$ were shown to lack symmetry.

In order to quantify the stability of the cluster ions, the calculated bonding energies were compared. Although the formation mechanism of the cluster ions proceeds via ionization and fragmentation of a neutral precursor, it is worthwhile to compare the assumed heat of formation estimated by calculation to obtain information about the relative stabilities of the cluster ion series. The calculated heats of formations using ADF (ZORA/TZP) were estimated as follows.

$$Sb_3O_4^+ + WO_3 \rightarrow Sb_3WO_7^+;\ \Delta H = -4.86\,\text{eV}$$

$$Sb_3WO_7^+ + WO_3 \rightarrow Sb_3W_2O_{10}^+;\ \Delta H = -3.51\,\text{eV}$$

$$Sb_3W_2O_{10}^+ + WO_3 \rightarrow Sb_3W_3O_{13}^+;\ \Delta H = -3.48\,\text{eV}$$

$$Sb_5O_7^+ + WO_3 \rightarrow Sb_5WO_{10}^+;\ \Delta H = -4.14\,\text{eV}$$

$$Sb_5WO_{10}^+ + WO_3 \rightarrow Sb_5W_2O_{13}^+;\ \Delta H = -3.68\,\text{eV}$$

$$Sb_5W_2O_{13}^+ + WO_3 \rightarrow Sb_5W_3O_{16}^+;\ \Delta H = -3.74\,\text{eV}$$

These estimations reveal that the addition of the WO_3 unit is always exothermic and that the Sb/W/O cluster ions are stabilized by the addition of WO_3. Among the series of $(Sb_3O_4)(WO_3)_n^+$ and $(Sb_5O_7)(WO_3)_n^+$ ($n = 0, 1, 2, 3$), the cluster ions $Sb_3WO_7^+$ and $Sb_5WO_{10}^+$ are more stable than the larger Sb/W/O cluster ions because the larger clusters have less exothermic enthalpies. These calculations are in agreement with our experimental results.

5. Conclusions

Sb/W/O clusters were produced by the oxidization of a W heater and Sb atoms in a gas-aggregation source. Sb/W/O cluster ions ionized by a 266-nm YAG laser were assigned to two series of cluster ions, $(Sb_3O_4)(WO_3)_n^+$ and $(Sb_5O_7)(WO_3)_n^+$, both of which have balanced numbers of free valence electrons and a total charge of +1. Among the Sb/W/O cluster ions, $Sb_3WO_7^+$ and $Sb_5WO_{10}^+$ were observed as very intense signals in the mass spectra, indicating their exceptional stability. The structures of the cluster ions were estimated using density-functional calculations. $Sb_3WO_7^+$ was calculated to have C_{3v} symmetry with a W atom opposite a six-membered ring consisting of three Sb and three O atoms. The W atom has a tetrahedral structure (WO_4) with one of the O atoms in a terminal position. In other Sb/W/O cluster ions, Sb and W tended to bond with three and four O atoms, respectively. The larger cluster ions had less symmetrical structures.

It was demonstrated that a W heater in the presence of O_2 can produce alloy oxide Sb/W/O clusters, and various kinds of tungstate cluster ions may be produced and studied by this method.

References

[1] K. Sattler, J. Möhlbach, P. Pfau, E. Recknagel, Phys. Lett. 87A (1982) 418.
[2] D. Rayane, P. Melinon, B. Cabaud, A. Hoareau, B. Tribollet, M. Broyer, Z. Phys. D 12 (1989) 217.
[3] C. Bréchignac, Ph. Cahuzac, F. Carlier, M. de Frutos, J. Leygnier, J.Ph. Roux, J. Chem. Phys. 102 (1995) 765.
[4] T.M. Bernhardt, B. Stegemann, B. Kaiser, K. Rademann, Angew. Chem. Int. Ed. 42 (2003) 199.
[5] D.M.P. Mingos, T. Slee, L. Zhenyang, Chem. Rev. 90 (1990) 83.
[6] B.V. Reddy, P. Jena, Chem. Phys. Lett. 288 (1998) 253.
[7] M. Kinne, T.M. Bernhardt, B. Kaiser, K. Rademann, Z. Phys. D 40 (1997) 105.
[8] M. Kinne, T.M. Bernhardt, B. Kaiser, K. Rademann, Int. J. Mass Spectrom. Ion Process. 167–168 (1997) 161.
[9] M.R. France, J.W. Buchanan, J.C. Robinson, S.H. Pullins, R.B. King, J.L. Tucker, M.A. Duncan, J. Phys. Chem. A 101 (1997) 6214.
[10] G. Ganteför, H.R. Siekmann, H.O. Lutz, K.H. Meiwes-Broer, Chem. Phys. Lett. 165 (1990) 293.
[11] B. Kaiser, T.M. Bernhardt, M. Kinne, K. Rademann, Int. J. Mass Spectrom. 177 (1998) L5.
[12] B. Kaiser, T.M. Bernhardt, M. Kinne, K. Rademann, A. Heidenreich, J. Chem. Phys. 110 (1999) 1437.
[13] M. Kinne, T.M. Bernhardt, B. Kaiser, K. Rademann, Int. J. Mass. Spectrom. Ion Process. 167–168 (1997) 161.
[14] J. Optiz-Coutureau, A. Fielicke, B. Kaiser, K. Rademann, Phys. Chem. Chem. Phys. 3 (2001) 3034.
[15] H.T. Deng, Y. Okada, M. Foltin, A.W. Castleman Jr., J. Phys. Chem. 98 (1994) 9350.
[16] G. Centi, S. Perathoner, Appl. Catal. A 124 (1995) 317.
[17] M. Bienati, V. Bonacic-Koutecky, P. Fantucci, J. Phys. Chem. A 104 (2000) 6983.
[18] C.D. Ling, R.L. Withers, A.D. Rae, S. Schmid, J.G. Thompson, Acta Cryst. B52 (1996) 610.
[19] C. Kaito, K. Fujita, M. Shiojiri, Jpn. J. Appl. Phys. 22 (1983) 252.
[20] Amsterdam Density Functional Program Package, Science Computing and Modeling NV, Vrije Universiteit, Theoretical Chemistry.
[21] E. van Lenthe, A.E. Ehlers, E.J. Baerends, J. Chem. Phys. 110 (1999) 8943.